RISK MANAGEMENT FOR SEISMIC RETROFIT OF A LONG-SPAN TRUSS BRIDGE APPLYING DAMAGE-CONTROLLED DESIGN

H. Kanaji
Hanshin Expressway Management and Technology Center, Japan
kanaji@tech-center.or.jp
Y. Fujino
University of Tokyo, Japan
fujino@civil.t.u-tokyo.ac.jp
T. Ishibashi
Hanshin Expressway Company Ltd., Japan
teruhisa.ishibashi@hanshin-exp.co.jp
T. Tokumasu
Ministry of Land, Infrastructure and Transport
tokumasu-k2uh@mlit.go.jp

ABSTRACT

The Minato Bridge is a long-span truss bridge with a length of 980m and located in the Hanshin Expressway at the Osaka Port, Japan. Although damage to this bridge from the 1995 Hyogo-ken Nanbu Earthquake had not been so serious, design seismic force for highway bridges was revised after the earthquake. Seismic performance of the bridge was evaluated by dynamic analysis applying revised ground motions and its seismic risk was found to be at non-negligible level. In this project, several types of retrofit structural systems with three different performance levels were considered and evaluated using seismic life-cycle cost (S-LCC). S-LCC consists of retrofitting cost and seismic risk. Several risks were calculated using the damage probability obtained from the hazard and fragility curves as well as cost data.

As a result, the damage-controlled structure with minimized S-LCC was employed to achieve rational retrofit from a view point of risk management. The concept was to differentiate main members which support vertical load from sub-members for lateral force such as seismic force. In this design, main members were required to be within linear region and sub-members were allowed to perform nonlinearly to provide damping. This structural system should allow early reopening of the bridge to traffic even after a severe earthquake so that it will serve as a part of lifeline and reduce social loss.

1. INTRODUCTION

The 1995 Hyogo-ken Nanbu Earthquake, which is commonly referred to as the Kobe earthquake, occurred on January 17, 1995, and its epicenter was in the northern part of Awaji-Island of Hyogo Prefecture. With the magnitude of 7.2, impacts from the prodigious earthquake were most serious in the Kansai region and further extended to wider areas from western to eastern Japan. Structures on the Kobe and Wangan routes in the Hanshin Expressway also suffered damage. There are long span bridges in the Wangan route, and some of which including the Higashi Kobe Bridge (cable-stayed bridge), Rokko Island Bridge (Lohse arch) and Nishinomiya-kou Bridge (Nielsen arch) were damaged to some extent.

The ministry of construction issued “Specifications for Restoration of Highway Bridges Damaged by the Hyogo-ken Nanbu Earthquake” immediately after the earthquake, and “Specifications for Highway Bridges, Part 5” and “Reference Book on Seismic Design of Highway Bridges” were reviewed and modified to take the damage into consideration and enhance ductility design. However, there were no specifications for seismic retrofit of long span bridges with span lengths exceeding 200m, and it was necessary to study performance of each bridge and establish seismic retrofit criteria and countermeasures.

The Minato Bridge, which was completed in 1974 and is located in Osaka, Japan, is a 980m-long cantilever-truss bridge. It is the third longest truss bridge in the world. The seismic capacity of this bridge was found to be not satisfying the new seismic design criteria established after the 1995 Kobe earthquake because it was originally designed for a ground acceleration of 250 gals. This bridge therefore needed to be retrofitted, and risk management for the retrofit was carried out in order to demonstrate the effectiveness of the retrofit and set a required performance level. This risk management also helps determine a rational structural system and implement damage controlled design. In this paper, risk management and seismic retrofit of the long-span truss bridge are introduced, and the cost benefit analysis and response reduction effects are also described.

2. OUTLINE OF THE BRIDGE AND SEISMIC RISK ASSESMENT

2.1. Bridge description

The Minato Bridge has a 510m central span composed of one suspended span and two 235m side spans as shown in Fig. 1. The bridge has double floor decks with 6 plate girders which were supported by conventional steel bearings on floor beams of the main truss. The weight of the two floor systems amounts to approximately 200MN, which accounts for 40% of the total weight of the superstructure.

A three-dimensional model of the whole bridge including the soil-foundation-structure interaction was prepared in order to evaluate the overall behavior of the bridge. The connections of main members such as chord, vertical and diagonal members supporting dead and live loads were modelled as rigid connections. The connection between cross beams including floor beams and the main members was modelled as pinned connection. Linear modal analysis using the three-dimensional computer model of the as-built structure was conducted to evaluate its vibration characteristics. Fig. 2 shows the dominant vibration modes for the longitudinal and transverse directions. Here, floor decks fixed to the main truss were assumed to vibrate altogether.

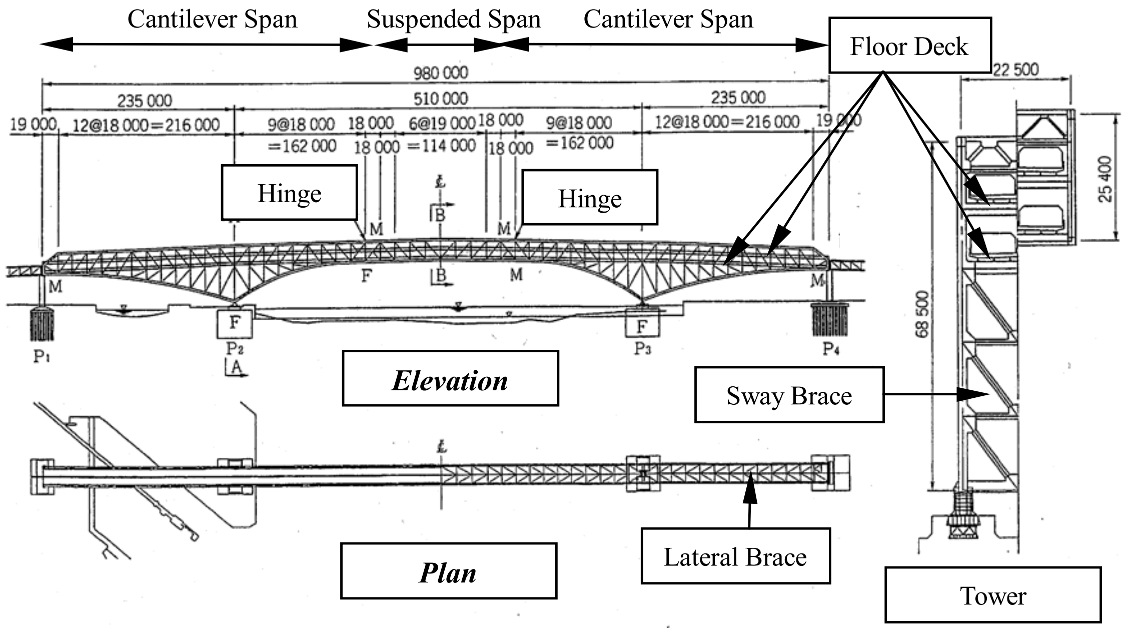

Fig. 1 - Structural characteristics of Minato Bridge

First Mode (T=2.8 sec.)

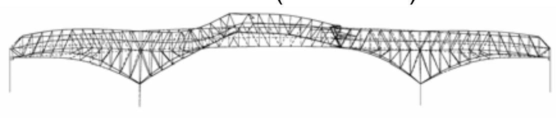

Second Mode (T=1.4 sec.)
a) Longitudinal Direction (Elevation)

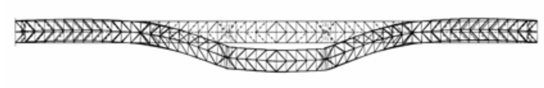

First Mode (T=4.4 sec.)

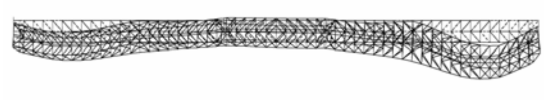

Second Mode (T=1.9 sec.)
b) Transverse Direction (Plan)

Fig. 2 - Dominant vibration modes for Minato Bridge

2.2. Lessons from the previous earthquake on seismic risk

There has been almost no report on damage to long-span bridges except for the Kobe earthquake. The Kobe earthquake which occurred in January 1995 damaged bridges in the Wangan and Kobe Routes of the Hanshin Expressway. The damage suffered by many long-span bridges in the Wangan Route was not minor. Some typical types of damage are described below.

The Minato Bridge has double decks in the main truss and decks, with a mass ratio of approximately 0.67. They had been supported by fixed bearings and movable bearings before the retrofit. There was no damage to the main truss; however, some deck bearings were damaged as shown in Fig. 3. This shows that the floor deck was isolated from the main truss by the failure of the existing bearings whose strength was smaller than those of the other structural elements. The bearing failure acted like a fuse.

a) Fracture of bearing stopper

b) Fracture of set bolts in bearing

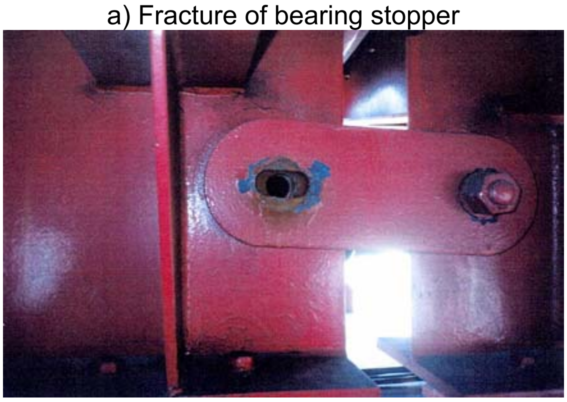

c) Bolt fracture of restrainer

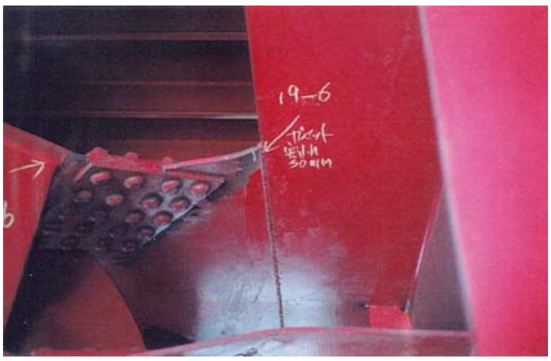

d) Damage to gusset plate

Fig. 3 - Damage on Minato Bridge

2.3. Seismic performance

Response spectrum analyses and time history analysis using the site-specific earthquake motions were carried out. It was found that the response acceleration spectrum for the first mode in the longitudinal direction was quite larger than that in the original design, suggesting that shifting the first natural period should be an effective solution. The natural period of the first mode in the transverse direction was adequately long, and increasing the damping was considered to be effective for the second mode.

A linear dynamic time history analysis was conducted to evaluate details of the seismic performance of the as-built structure. As a result, some members were found to be not satisfying the basic allowable demand/capacity ratio, R_{req} = 1.0. Demand/capacity ratio R_i for each member is defined as follows.

$$R_i = \sigma_{\max_i} / \sigma_{a_i}$$

where, $\sigma_{\max_i}$ = Maximum member stress obtained by dynamic analysis (i = 1,2,…, total number of members), σ_{a_i} = Allowable (yield or buckling) member stress (i = 1,2,…, total number of members)

Fig. 4 shows distribution of R_i for all members. It can be stated that yielding ($R< -1.0$) or buckling ($R>1.0$) occurs in chord members located near the edges of side-spans, and around hinges between the cantilever span and the suspended span due to the longitudinal response. Inelastic behaviour would occur in the chord members located near the edges of the bridge, in the lower chord, diagonal or vertical members of the side-spans near the towers, and in towers' diagonal members due to the transverse response. Therefore these members need to be retrofitted or provided with some measures to reduce seismic responses.

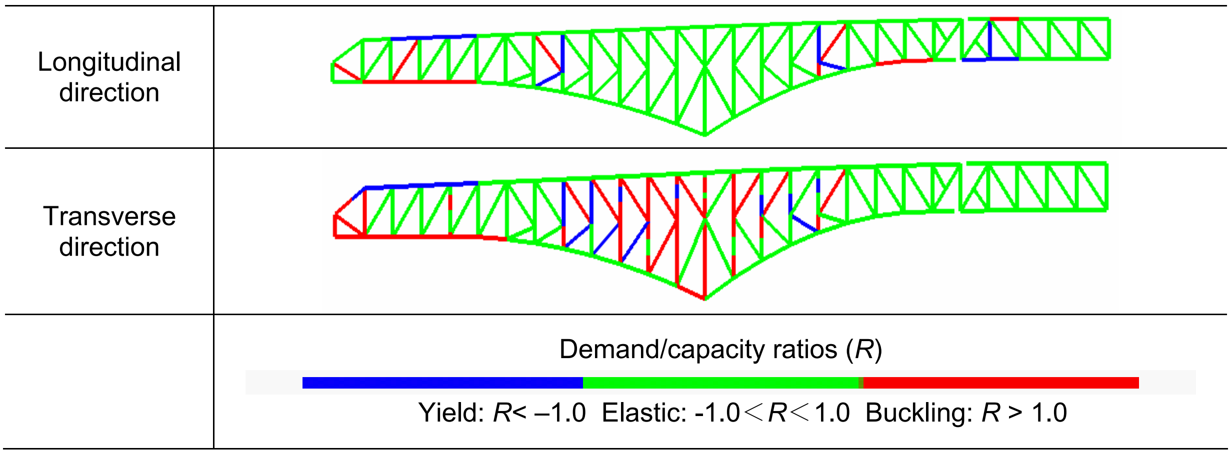

Fig. 4 - Demand/capacity ratios

3. RISK MANAGEMENT FOR RETROFIT STRATEGY

3.1. Risk management and LCC

It is important to determine the best combination of design seismic load and structural performance where most rational investment is achieved. Therefore various sorts of structural systems should be studied by cost-benefit analysis. After risks are specified and evaluated through risk management, choices are made from mitigation, retention, transfer or evasion. We can say that the selection of the best structural system based on cost-benefit analysis for seismic retrofit is sort of it.

Retrofit of long-span bridges is generally behind schedule because it involves enormous cost, advanced technologies and large-scale construction. We have to fulfil accountability for investing quite a large sum of money. In this study, life-cycle costs were determined for several retrofit structural systems, and the best structure was selected from a view point of LCC. The purpose of retrofit is to reduce risks by investments. The benefit is the differential between risks before and after retrofit. LCC was calculated based on the flow chart shown in Fig. 5.

Seismic risk analysis was conducted to generate hazard spectra and design accelerograms. Three-D analysis was carried out to determine stress ratios for all structural members, and 3-D finite element method analysis was carried out to evaluate the relationship between damage states and loads. Based on these results with material variations taken into account, fragility curve was obtained. Damage probability was calculated by correlating stress ratios of all members with the fragility curve, and rank-by-rank loss was obtained. In this study, we assumed 3 levels from Levels 1 to 3 for retrofit strategy. Here, total loss was obtained as follows.

$$C_f = \int_p C_f(p)dp$$

where $C_f(p)$=total loss at exceedance probability p

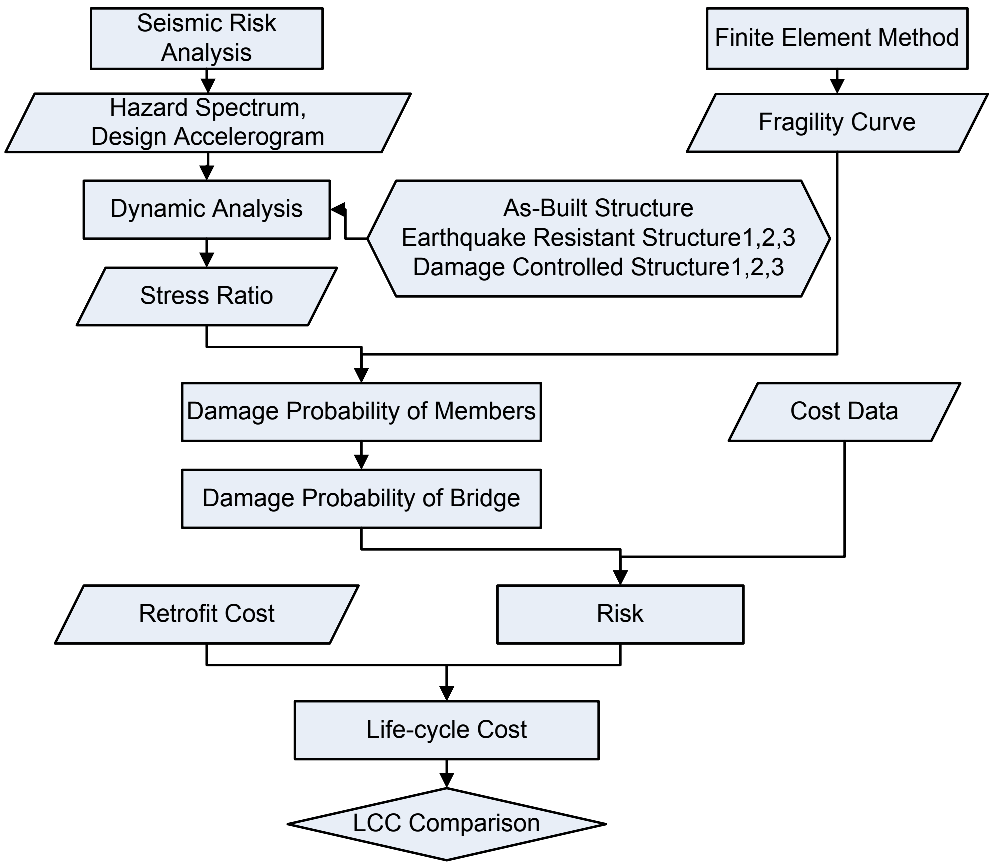

Fig. 5 - Flow of risk management

3.2. Performance criteria

Basic performance levels are described in Table 1. In this table, two structural systems are described: earthquake resistant structure (ERS) and damage controlled structure (DCS). Level 1 is the full performance level for the structure without considering the retrofit cost where all structural elements should be within elastic region even during a severe earthquake. Level 2 is the moderate performance level where non-main truss members such as sway bracings or lateral bracings may yield but only to a repairable condition. Level 3 is the lowest for retrofit work where main truss and non-main truss may suffer severe damage which involve enormous reconstruction or repair cost. In order to determine the best performance of this bridge with both retrofit cost and risk taken into account, we have estimated seismic life-cycle cost. The risk consists of loss of life, loss of toll revenue, time loss and restoration cost.

Table 1 - Performance Requirements and Criteria

Level	Performance Requirements of the bridge	Performance Criteria for Earthquake Resistant Structure (ERS)	Performance Criteria for Damage Controlled Structure (DCS)
1	-Fatal accident / bridge collapse avoided -Immediately reopened to service	-All members should be essentially elastic.	-All members should be essentially elastic. -Damage controlled device provides damping.
2	-Fatal accident / bridge collapse avoided -Almost immediately reopened to service	-Main truss should be elastic, although damage to non-main truss may be allowed	-Main truss should be elastic, although damage to non-main truss may be allowed -Damage control device provides damping.
3	-Fatal accident / bridge collapse avoided (Rebuilding, repair or reinforcement are needed)	-Damage to any members may be allowed but without collapse.	-Damage to any members may be allowed but without collapse. -Damage control device provides damping.

3.3. Hazard curve

Fig. 6 shows 4 hazard curves which represent relationships between period and response acceleration for the bridge site: 50 years exceedance probability p=0.02, 0.05, 0.10 and 0.39. The probability p=0.05 corresponds to a 1000 year return period which is the maximum credible earthquake period.

3.4. Fragility curve

Finite element method was applied to evaluate the elasto-plastic performance of damaged members of the bridge. The models for them were generated in three-dimensions with actual conditions such as loading combination, constraint state and initial defects taken into account. The load-displacement relationship was obtained from the analysis, and correlations were made between stress ratio and damage condition.
Elastic limit was reached at a stress ratio of 1.2, and ultimate state was reached at 1.5. These stress ratios were adopted as the thresholds for damage ranks ”a” and ”a_s”, respectively. In this study, we used actual yield strength of members, not normal yield strength. The ratio of the average actual strength to the nominal strength was 1.15. The strength standard variation applied was 0.13, and the standard variation of the ultimate strength was considered as 0.26, because the ultimate strength from the FEM analysis varied significantly.

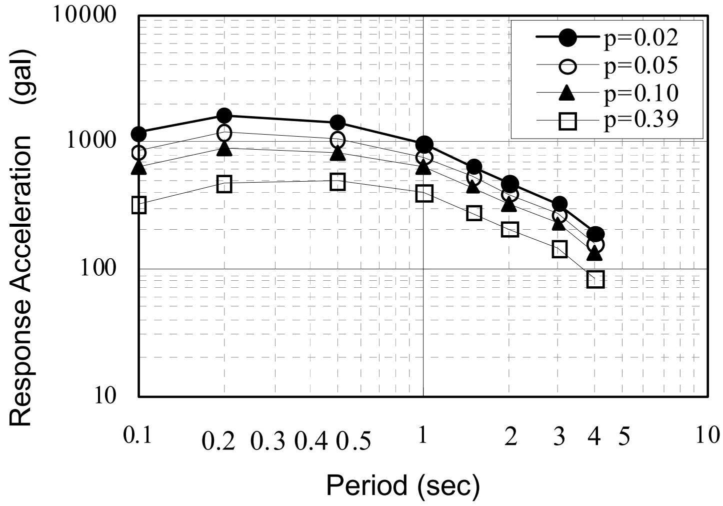

Fig. 6 - Hazard curve

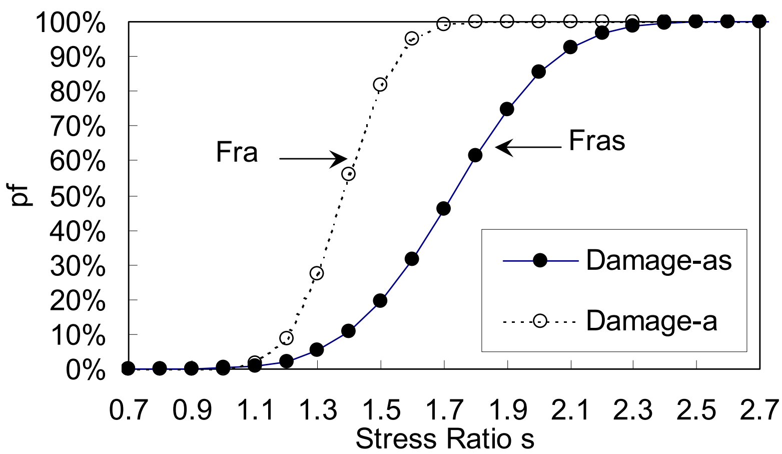

Fig. 7 - Fragility curve

3.5. Damage probability

Damage probability of each member was obtained from the following equation.

$$p_{fki} = Fr_k(R_i)$$

where p_{fki}=damage probability of member *i* for damage rank k, R_i=stress ratio of member *i* , Fr_k=fragility function for rank *k*

Failure or severe damage of one main truss member such as a chord member, a vertical member or a diagonal member will result in the bridge failure, because the intended bridge is the statically determinate structure. Therefore damage probability of the bridge for rank A_s is expressed by the following equation.

$$P_{fs} = \sum_{i=1}^{n} p_{fsi}$$

where P_{fs}=damage probability of rank A_s for the bridge, p_{fsi}=damage probability of rank a_s for member *i*

$$P_{fa} = \sum_{i=1}^{n} \hat{p}_{fai}$$

where P_{fa}=damage probability of rank A for the bridge, $\hat{p}_{fai}$ = failure probability of rank a for member i without a_s damage in other members

Fig. 8 shows the relationship between the maximum acceleration and the damage probability and provides the result of the above-mentioned calculation for ranks A_s and A of as-built structure and retrofitted structure. In case of p=39% corresponding to 100 year return period, the probability of A_s was very small for both structures. In case of p=5% corresponding to 1000 year return period, the probability of A_s for the as-built structure was almost 100%, while that for the retrofitted structure was still very small. This demonstrates that the retrofit should be very effective for the bridge.

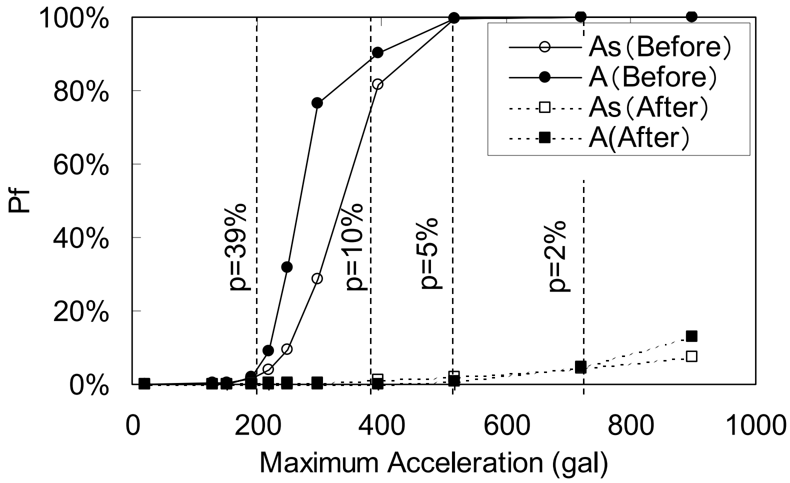

Fig. 8 - Damage probability for the bridge

3.6. Risk management based on seismic life-cycle cost

Losses to be analyzed include not only the restoration cost but also toll revenue loss (operating loss), human loss and economical loss from bridge closure after a severe earthquake. In this study, only travel time loss was considered as economical loss. Thus the total loss can be expressed as follows.

$$C_f = C_T + C_R + C_L + C_U$$

$$C_T = C_{Ts} \cdot P_{fs} + C_{Ta} \cdot P_{fa}$$

$$C_R = C_{Rs} \cdot P_{fs} + \sum_{i=1}^{n} (C_{Rai} \cdot p_{fai})$$

$$C_L = C_{Ls} \cdot P_{fs}$$

$$C_U = C_{Us} \cdot P_{fs} + C_{Ua} \cdot P_{fa}$$

where C_f=total loss, C_T=toll revenue loss, C_R=restoration cost, C_L=human loss, C_U=travel time loss, C_{Ts}=toll revenue loss from damage A_s, C_{Ta}=toll revenue loss from damage A, C_{Rs}=restoration cost due to damage A_s, C_{Rai}=rehabilitation cost of member *i* with damage a, C_{Ls}=human loss from damage A_s, P_{fs}=damage probability of damage As, P_{fa}=damage probability of damage A, p_{fai}=damage probability of damage a for member *i*, C_{Us}=travel time loss from damage A_s , C_{Ua}=travel time loss from damage A

In order to calculate each cost, restoration procedure, unit price, bridge closure time and other factors were set in advance. Table 2 and Table 3 show the damage ranking, restoration policies, and their cost data. The average toll rate was set as 700 yen/vehicle for the toll revenue loss calculation using the actual toll rate for standard-sized cars.

Table 2 - Damage ranking and restoration

Damage Rank		Restoration	Unit cost (million yen)	Bridge closure time
A_s		Reconstruction	See Table 3	3 years
A	Main truss	Repair & rehabilitation	0.45/ton	1.46 days/ton
	Sub member	Replacement	1.0/ton	N/A

Table 3 - Construction (Reconstruction) cost and deflator

Time point	Construction cost (million yen)	Deflator
Construction (1972)	14,380	35.6
Present (2002)	39,303 (= C_{R0})	97.3

For the ultimate goal to evaluate the best structural system and performance level, we estimated the seismic life-cycle cost for each case using the following equation in which the present discounted value for future risk by social discount rate was taken into account.

$$LCC = C_{ug} + \sum_{i=1}^{N} \left(\frac{C_f}{N} \cdot \frac{1}{(1+r)^i} \right)$$

where C_{ug}=retrofit cost, C_f=total risk, *N*=evaluation period, 50 years, *r*=social discount rate, 4%, *i*=number of years

In Fig. 9 the normalized LCC by the present construction cost C_{R0} resulting from the seismic life-cycle cost analysis is displayed for each case. As can be seen, both retrofitted structures which were the earthquake resistant structure (ERS) and the damage controlled structure (DCS) with any performance levels reduced the normalized LCC dramatically as compared to the as-built structure. This figure indicates that the minimum normalized LCC is achieved in DCS-Level 2, showing the rationality and effectiveness of retrofitting the structure using this structural system to this performance level from a view point of risk management.

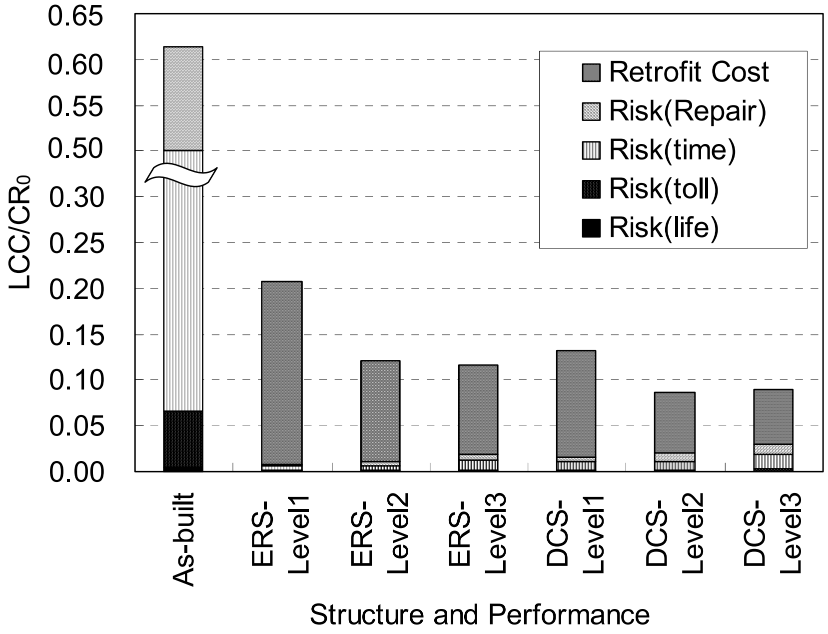

Fig. 9 - Normalized life-cycle cost

4. SEISMIC RETROFIT USING DAMAGE CONTROLLED DESIGN

4.1. Floor deck isolation

A sliding isolation system consisting of sliding bearings and lateral rubber springs was adopted for the floor deck isolation as shown in Fig. 10. The seismic isolation is based on period elongation by the rubber springs; consequently the natural period based on the stiffness of the rubber springs is critical for both member force of the main truss and displacement of the floor decks. Moreover, the friction coefficient of sliding bearings also affects the isolation system response. Therefore a parametric study was conducted to calculate optimal design values with member forces and displacements taken into account, by using time-history analysis.

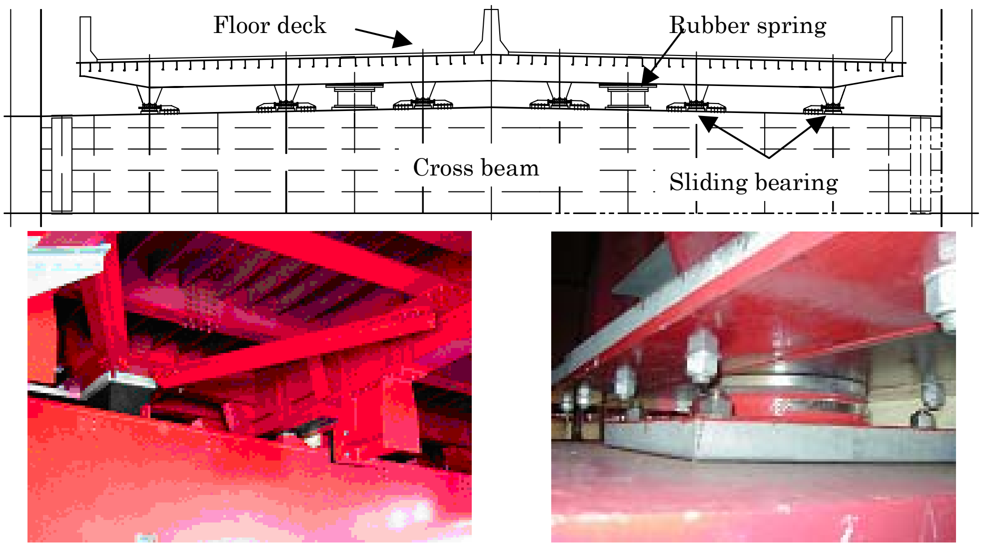

Fig. 10 - Floor deck seismic isolation system using sliding bearings

4.2. Buckling restrained brace

Steel hysteretic damper treated herein is called buckling restrained brace (hereinafter called BRB) and consists of low yield-point core steel (LY225) and outer steel which restrains the buckling of core steel as shown in Fig. 11. Although normal brace cannot provide hysteretic damping under cyclic loading because of buckling, BRB can give quite large damping without buckling. In order to give adequate damping to the entire bridge and also to avoid buckling or yielding of main members, the existing braces could be replaced by BRBs.

Based on the strain energy ratios obtained for all truss members by general modal analysis, we decided to replace the braces with BRBs with larger strain energy to increase the modal damping. With these results and performance criteria taken into account, lower lateral braces near the edges (Part_1) and towers (Part_2), and towers' sway braces (Part_3) were studied for replacement with BRBs as shown in Fig. 12. Consequently, BRBs in Part_2 and Part_3 were selected from the efficacy point of view.

Fig. 11 - BRB

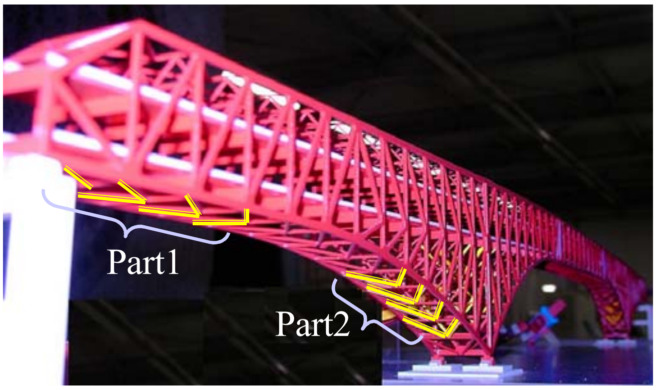

a) Lower lateral in side span

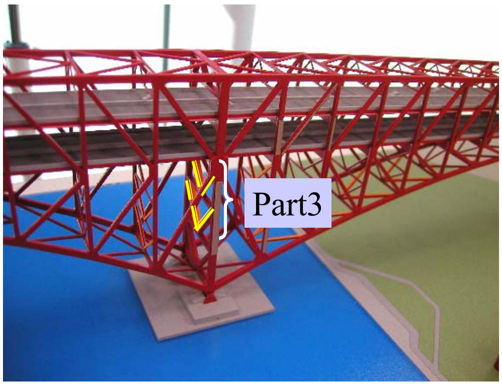

b) Tower brace

Fig. 12 - BRB layout

4.3. Retrofit performance

Time history analyses using the same design acceleration applied in the assessment of the as-built structure were conducted to confirm the effect of floor seismic isolation and BRB. From the demand/capacity ratio shown in Fig. 13, it was clear that the number of yielding or buckling members was smaller than that of the as-built structure shown in Fig. 4. It demonstrates that floor seismic isolation and BRB dramatically reduce the member force. In addition, they reduce the residual deformation of the whole bridge and prevent the vulnerable hinges at the center span from diddling.

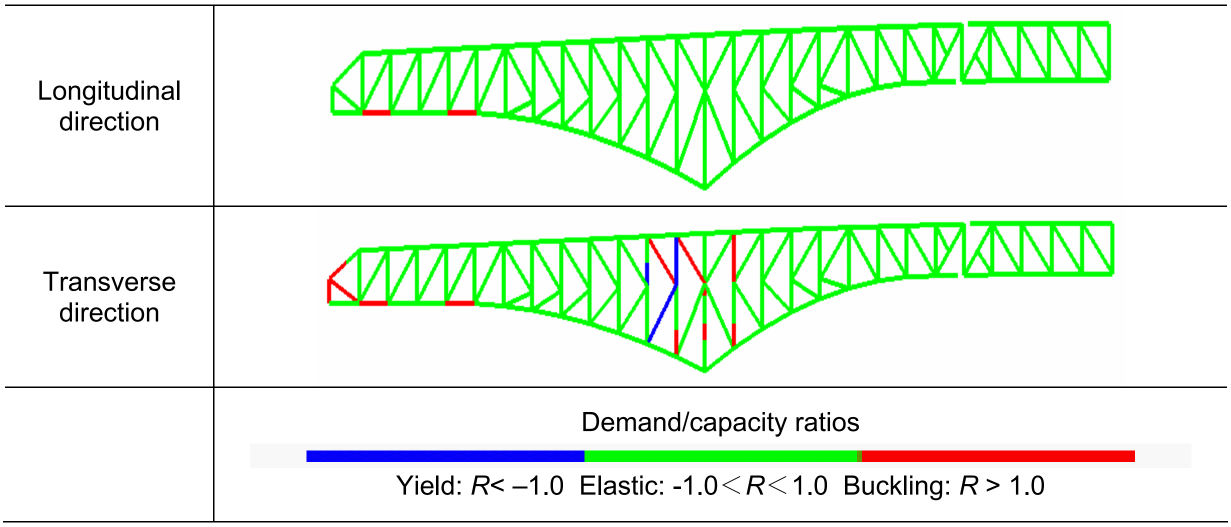

Fig. 13 - Demand/capacity ratio after retrofit

5. CONCLUSIONS

From this study, it is possible to conclude as follows:

1) The damage-controlled structure with the most minimized S-LCC was employed to achieve the innovative retrofit from a view point of risk management. The concept was to differentiate main members that support vertical load from sub-members for lateral force such as seismic force.
2) In this design, main members were required to be within linear region and sub-members were allowed to perform elasto-plastic behaviour to provide damping. This structural system should allow early reopening of the bridge to traffic even after a severe earthquake so that it will serve as a part of lifeline and reduce social loss.
3) Floor deck isolation and buckling restrained braces based on damage control design were found to be very effective solutions for the retrofitting of the long-span bridge with the dynamic response of the whole bridge being reduced considerably.

REFERENCES

1. Eiichi Watanabe, Hirokazu Iemura, Hidesada Kanaji, Tsutomu Nishioka and Takumi Ohyama : New Japanese Technological Contributions for Earthquake Engineering, Proc. of the 6th TRB International Bridge Engineering Conference, July 17-20, 2005.
2. Hidesada Kanaji, Yozo Fujino, Eiichi Watanabe, Naoto Suzuki : Seismic Retrofit of a Long-span Truss Bridge applying Damage Control Strategy, Proc. of the International Association for Bridge and Structural Engineering Conference, Copenhagen, Denmark, May 15-17, 2006.